

Cite this: DOI: 00.0000/xxxxxxxxxx

Temperature effects on the ionic conductivity in concentrated alkaline electrolyte solutions[†]Yunqi Shao,^a Matti Hellström,^{b,c} Are Yllö,^a Jonas Mindemark,^a Kersti Hermansson,^a Jörg Behler,^b and Chao Zhang^{*a}

Alkaline electrolyte solutions are important components in rechargeable batteries and alkaline fuel cells. As the ionic conductivity is thought to be a limiting factor in the performance of these devices, which are often operated at elevated temperatures, its temperature dependence is of significant interest. Here we use NaOH as a prototypical example of alkaline electrolytes, and for this system we have carried out reactive molecular dynamics simulations with an experimentally verified high-dimensional neural network potential derived from density-functional theory calculations. It is found that in concentrated NaOH solutions elevated temperatures enhance both the contributions from proton transfer to the ionic conductivity and deviations from the Nernst-Einstein relation. These findings are expected to be of practical relevance for electrochemical devices based on alkaline electrolyte solutions.

Because of their excellent ionic conductivity and high room-temperature solubility, alkaline electrolyte solutions are widely used in electrochemical devices such as rechargeable batteries and alkaline fuel cells^{1,2}. The electrochemically active ion in alkaline electrolytes is the hydroxide ion³. OH⁻ has an anomalously high mobility in aqueous solution, as it can diffuse via Grotthuss mechanism which is composed of a series of proton transfer events⁴. Major progress in the understanding of OH⁻ solvation and mobility at low concentration was made by molecular dynamics (MD) simulations based on density functional theory⁵⁻⁹ and reactive force fields¹⁰⁻¹², which highlighted the importance of “presolvation”, i.e., a thermally induced hydrogen-bond fluctuation, in the diffusion of hydroxide ions^{7,10-13}.

Although ionic conductivity at low concentrations is well-described by the Nernst-Einstein equation, which links the conductivity σ to the self-diffusion coefficients D_+ and D_- of cations

and anions, respectively, this simple picture is no longer valid at concentrations typically used in electrochemical devices. At higher concentrations, several types of non-ideal phenomena like ion-pairing¹⁴, in which cations and anions associate and form metastable neutral pairs, and, more generally, cross-correlations of the movements of different ions (of equal or opposite charge) can notably alter the ionic conductivity. Moreover, the working temperature of alkaline batteries and fuel cells can be much higher than room-temperature (293K)¹⁵. Therefore, it is desirable to understand the temperature effect on proton transfer and ion-pairing in alkaline electrolyte solutions and their implications concerning the ionic conductivity at high concentrations and elevated temperatures.

Simulations of electric properties, such as ionic conductivity, necessitate long timescales and, except for cases at extreme conditions¹⁶, are normally beyond reach of density functional theory-based MD. One way to tackle this time-scale challenge is to explore finite-field methods to speed up the convergence of the polarization \mathbf{P} , which has been successfully applied to compute the dielectric constant of polar liquids and the capacitance of electrified solid-electrolyte interfaces¹⁷. The other approach to solve this problem is to make use of reactive force fields to access longer time-scales^{12,18}. One promising approach in this direction is to devise high-dimensional neural network potentials (NNPs) with density-functional theory (DFT) quality as proposed by Behler and Parrinello¹⁹. Here, we use this approach, and by means of molecular dynamics (MD) simulations using a NNP for the prototypical case of aqueous NaOH solutions²⁰ and show how different factors in together lead to the surprising behavior of the ionic conductivity in concentrated NaOH aqueous solutions at elevated temperatures.

The details of the construction and validation of our NNP for NaOH solutions using DFT calculations at the dispersion-corrected GGA level have been discussed in Ref. 20. The MD simulations were performed using LAMMPS²¹ together with an extension for high-dimensional NNPs²². The cubic simulation box contained between 272 and 496 water molecules, and between 8 and 120 NaOH formula units, depending on concentration (see Table S1 in the ESI[†]). The length of cubic simulation box has been fixed using the experimental densities of NaOH solutions at the given composition and temperature²³ (see Table S1 in the

^a Department of Chemistry - Ångström Laboratory, Uppsala University, Box 538, 751 21 Uppsala, Sweden; Email: chao.zhang@kemi.uu.se

^b Universität Göttingen, Institut für Physikalische Chemie, Theoretische Chemie, Tammannstr. 6, 37077 Göttingen, Germany

^c Software for Chemistry and Materials B.V., De Boelelaan 1083, 1081HV Amsterdam, The Netherlands

[†] Electronic Supplementary Information (ESI) available: [details of any supplementary information available should be included here]. See DOI: 00.0000/00000000.

ESI†). Production runs with a timestep of 0.5 fs in the *NVT* ensemble lasted for 15 ns at each combination of composition and temperature after the equilibration. The Bussi-Donadio-Parrinello thermostat²⁴ which has shown an excellent control of kinetic energy and little effect on the dynamical properties was employed. The trajectory frames were saved every 0.01 ps for later analysis. Each trajectory was split into 5 uncorrelated segments with length of 3 ns each. The standard deviations of observables from the different segments were used as an error estimate. Note that nuclear quantum effects were not included in the MD simulations.

To accompany the simulations, we have also performed conductivity measurements of NaOH solutions of concentrations up to 25 molality (m) using an "InLab" conductivity meter (Mettler Toledo). The conductivity meter probe used is a 4 pole InLab 738-ISM by (Mettler Toledo) which has a sensitivity range from 0.01–1000 mS cm⁻¹ and gives accurate measurements up to 373K. The mean and the standard deviation of five independent measurements after calibration were reported for each given NaOH solution at both 293K and 323K.

When comparing simulation and experimental results, it is important to realize that the ionic conductivity can be computed using different formulas which have different applicabilities. As mentioned at the beginning, the Nernst-Einstein equation for the ionic conductivity of a 1:1 symmetric electrolyte is valid only at low concentration and can be written as

$$\sigma_{N-E} = q^2 \rho \beta (D_+ + D_-), \quad (1)$$

where β is the inverse temperature, q is the formal charge of each ion and ρ is the number density of the formula unit of 1:1 electrolyte.

D_+ can be obtained by integrating the velocity auto-correlation function as

$$D_+ = \frac{1}{3} \int_0^\infty dt \langle \mathbf{v}_{i,+}(0) \mathbf{v}_{i,+}(t) \rangle \quad (2)$$

where t is time and $\mathbf{v}_{i,+}$ is the velocity vector of the i th cation, and the average is taken over all cations and time origins. Alternatively, the Einstein relation

$$D_+ = \lim_{t \rightarrow \infty} \frac{1}{6t} \langle [\mathbf{r}_{i,+}(t) - \mathbf{r}_{i,+}(0)]^2 \rangle \quad (3)$$

can be used, where $\mathbf{r}_{i,+}$ is the position of the i th cation.

D_- can be computed analogously according to Eqs 2 and 3. We defined the positions of OH⁻ ions by the position of O atoms bonded only to a single H atom. All bonds in the system were defined by assigning each hydrogen atom to its nearest oxygen atom, which gave either water molecules or hydroxide ions. Upon proton transfer reactions, the trajectories of OH⁻ were traced in a fashion similar to how was done in Ref. 25, i.e. based on "the Hungarian algorithm" as introduced by König in 1916 and Egerváry in 1931 and elaborated by Kuhn in 1974²⁶.

The Nernst-Einstein equation becomes approximate at high concentrations, for which ion-pairing and cross-correlated ion motions play an important role^{27–29}. A more general equation for the conductivity, which is valid at both low and high concen-

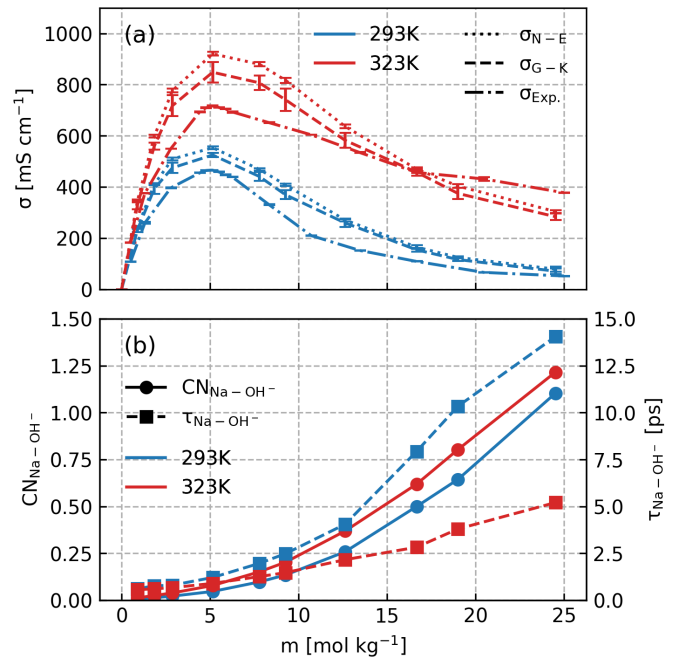


Fig. 1 (a) Comparison of concentration-dependent ionic conductivities calculated using the Nernst-Einstein formula (Eq. 1 and Eq. 3) and the Green-Kubo formula (Eq. 5) from MD simulations and those measured in experiments at 293K and 323K; (b) Calculated Na⁺–OH⁻ coordination numbers and residence time.

tration, is the Green-Kubo formula

$$\sigma_{G-K} = \frac{\beta}{3} \int d\mathbf{r} \int_0^\infty dt \langle \mathbf{J}(0) \mathbf{J}(t) \rangle \quad (4)$$

where \mathbf{J} is the current density. Alternatively, the equivalent Einstein-type relation can also be used³⁰

$$\sigma_{G-K} = \lim_{t \rightarrow \infty} \frac{\beta \Omega}{6t} \langle [\mathbf{P}(t) - \mathbf{P}(0)]^2 \rangle \quad (5)$$

where \mathbf{P} is the itinerant polarization in ionic solution³¹ and Ω is the volume of the simulation box.

Unlike σ_{N-E} , σ_{G-K} includes ion-pairing and cross-correlated ion motions from the so-called distinct diffusion coefficients of cations D_+^d , anions D_-^d and cation-anion pairs D_{+-}^d , which can be computed from MD simulations^{28,32}. The name "distinct" means it is cross-correlation between two different ions, even within the same species.

This leads to a decomposition of the Green-Kubo conductivity as

$$\sigma_{G-K} = q^2 \rho \beta (D_+ + D_- + D_+^d/2 + D_-^d/2 - D_{+-}^d) \quad (6)$$

$$= \sigma_{N-E} + \sigma_+^d + \sigma_-^d + \sigma_{+-}^d \quad (7)$$

where σ_+^d , σ_-^d and σ_{+-}^d are contributions to the ionic conductivity from the corresponding distinct diffusion coefficients.

After elaborating on the difference between the Nernst-Einstein conductivity and the Green-Kubo conductivity, we are now ready to compare the ionic conductivity calculated from MD simula-

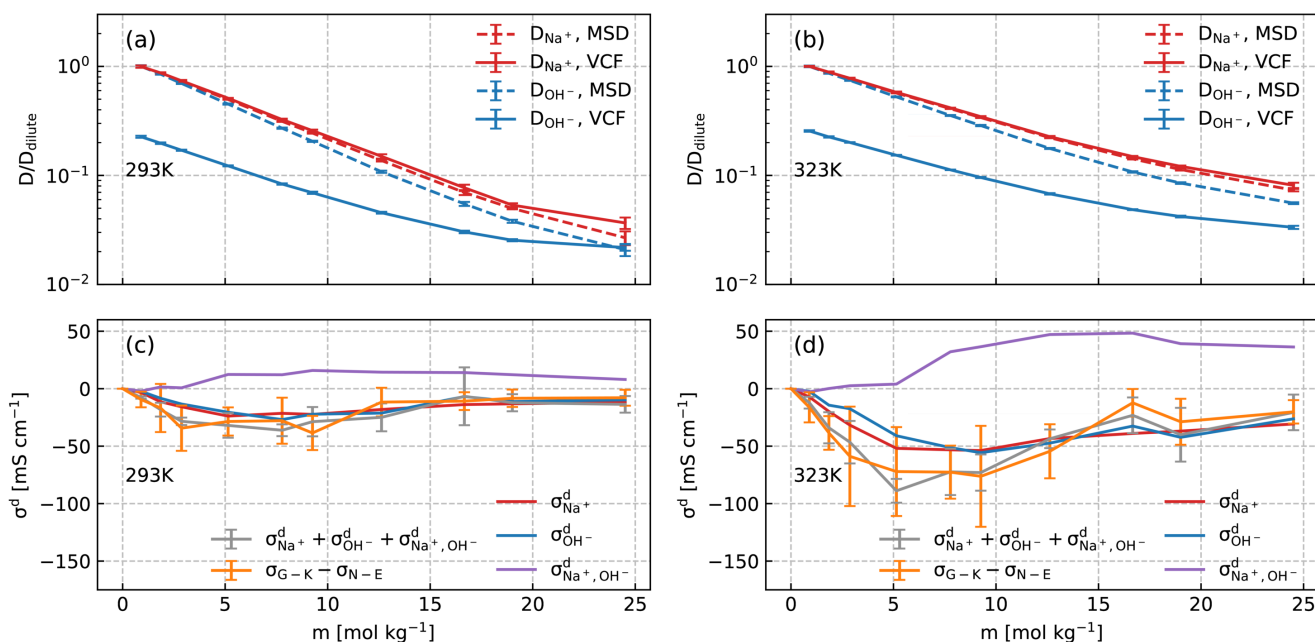


Fig. 2 (a) and (b) Scaled concentration-dependent self-diffusion coefficients of Na^+ and OH^- at 293K and 323K obtained from VCF (Eq. 2) and from MSD (Eq. 3), where the self-diffusion coefficients were scaled by the corresponding value in the dilute solution; (c) and (d) Contributions from distinct diffusion coefficients to the ionic conductivity at 293K and 323K as shown in Eq. 7 and calculated from VCFs. Detailed definition of distinct diffusion coefficients can be found in Ref. 28,32.

tions to those measured in experiments. The results are shown in Fig. 1. In Fig. 1a, the calculated ionic conductivities from MD simulations agree well with conductivity measurements, especially at 293K. Considering that the NNP²⁰ was generated using only DFT calculations as the reference, this agreement is quite encouraging. Note that we have neglected the finite-size correction³³ to the Nernst-Einstein conductivity showed in Fig. 1a, because of the relatively large simulation box that we used and the high viscosity of concentrated NaOH solutions (See Fig. S1 in the ESI†).

When inspecting the simulation results at both 293K and 323K (Fig. 1), one can see that the Nernst-Einstein conductivity is always larger than the Green-Kubo conductivity, as expected. However, there are several interesting observations specific to NaOH solutions. First, the absolute difference between the Nernst-Einstein conductivity and the Green-Kubo conductivity becomes smaller at higher concentrations which is counter-intuitive. Second, the difference is in general larger at higher temperature (323K) than at lower temperature (293K). Third, near the solubility limit (25 m) at room-temperature, the ionic conductivity at 323K is still substantial while at 293K it becomes quite small.

One way to rationalize these observations is to consider ion-pairing. For this reason, we calculated the coordination number of OH^- around Na^+ ions as well the residence time of $\text{Na}^+ - \text{OH}^-$ pairs. The coordination number was calculated by integrating the radial distribution function to its first minimum and the residence time was calculated by following the stable states picture formalism³⁴. As is described in Ref 35, a time correlation function $C(t)$ was calculated to give the probability that a "stable" hydroxide ion at time t does not escape the first coordination shell of Na^+

through either ligand exchange or proton transfer within the interval t_0 and $t_0 + t$. $C(t)$ was then fitted to a biexponentially decaying function to extract the residence time. As shown in Fig. 1b, the number of OH^- coordinating Na^+ at both 293K and 323K can exceed one near the room-temperature solubility limit. However, the residence time at 293K increases much more rapidly with the concentration than that at 323K. Based on these observations, we speculate that the effect of ion-pairing on the ionic conductivity would be stronger at 293K.

In order to dissect contributions from proton transfer reactions and cross-correlated ion motions, we exploited the fact that proton transfer contributes to the mean squared displacement (MSD, Eq. 3) but not to the corresponding velocity correlation function (VCF, Eq. 2). As shown in Fig. 2a and Fig. 2b, the scaled self-diffusion coefficients of Na^+ are the same regardless whether they are computed from MSD or from VCF. In contrast, the scaled self-diffusion coefficients of OH^- computed from MSD and VCF are different and their difference quantifies the contribution from proton transfer reactions. Comparing to the case at 323K, one can clearly see that the proton transfer contribution to the self-diffusion coefficient of OH^- becomes negligible at 293K in concentrated NaOH solutions. This is the main reason why the ionic conductivity near the room-temperature solubility limit at 323K is still significant while at 293K it becomes severely diminished.

We then used the same technique to evaluate the contributions from the distinct diffusion coefficients to the ionic conductivity from VCFs, as shown in Fig. 2c and Fig. 2d. It is found that $\sigma_{\text{Na}^+, \text{OH}^-}^d$ at both 293K and 323K are positive instead of negative as a simple picture of ion-pairing would suggest. Further,

$\sigma_{\text{Na}^+, \text{OH}^-}^{\text{d}}$ is much more positive at 323 K than that at 293 K. If one considers that the negativeness of $\sigma_{\text{Na}^+, \text{OH}^-}^{\text{d}}$ as the onset of ion-pairing contributions to the ionic conductivity, then the effect of ion-pairing on the ionic conductivity are more likely to happen at 293 K than that at 323 K.

When comparing the sum of $\sigma_{\text{Na}^+}^{\text{d}}$, $\sigma_{\text{OH}^-}^{\text{d}}$ and $\sigma_{\text{Na}^+, \text{OH}^-}^{\text{d}}$ calculated from VCFs to the absolute difference between $\sigma_{\text{G-K}}$ and $\sigma_{\text{N-E}}$ calculated from the MSD, one can see a good agreement within the statistical error. Note that $(\sigma_{\text{G-K}} - \sigma_{\text{N-E}})$ has a larger error bar than its counterpart $(\sigma_{\text{Na}^+}^{\text{d}} + \sigma_{\text{OH}^-}^{\text{d}} + \sigma_{\text{Na}^+, \text{OH}^-}^{\text{d}})$, because the former is the difference of two large numbers (Fig. 1a). The agreement between these two quantities means that the cross-correlated ion motions are hydrodynamic in nature and not determined by proton transfer reactions in NaOH solutions. We suspect that the counter-intuitive observation that $(\sigma_{\text{G-K}} - \sigma_{\text{N-E}})$ becomes smaller at high concentration is related to the rapid increment of the viscosity in NaOH solutions (See Fig. S2 in the ESI†). Since the viscosity decreases at elevated temperatures, this may also explain a larger difference between the Nernst-Einstein conductivity and the Green-Kubo conductivity at 323K as seen in Fig. 1a. Nevertheless, future investigations are needed to identify the factors affecting the cross-correlated ion motions and subsequent deviations from the Nernst-Einstein relation³⁶.

Conflicts of interest

There are no conflicts to declare.

Acknowledgements

CZ thanks Uppsala University (UU) for a start-up grant and funding from the Swedish National Strategic e-Science programme eSENCE. MH acknowledges funding from the European Union's Horizon 2020 research and innovation programme under grant agreement No 798129. JB acknowledges the DFG for a DFG Heisenberg professorship (Be3264/11-2, project 329898176). The simulations were performed on the resources provided by the Swedish National Infrastructure for Computing (SNIC) at NSC.

Notes and references

- 1 G. Merle, M. Wessling and K. Nijmeijer, *J. Membr. Sci.*, 2011, **377**, 1–35.
- 2 A. R. Mainar, O. Leonet, M. Bengoechea, I. Boyano, I. de Meaza, A. Kvasha, A. Guerfi and J. Alberto Blázquez, *Int. J. Energy Res.*, 2016, **40**, 1032–1049.
- 3 E. Hückel, *Z. Elektrochem. Angew. Physik. Chem.*, 1928, **34**, 546–562.
- 4 N. Agmon, *Chem. Phys. Lett.*, 1995, **244**, 456–462.
- 5 M. E. Tuckerman, K. Laasonen, M. Sprik and M. Parrinello, *J. Phys.: Condens. Mat.*, 1994, **6**, A93–A100.
- 6 M. E. Tuckerman, D. Marx and M. Parrinello, *Nature*, 2002, **417**, 925–929.
- 7 D. Marx, A. Chandra and M. E. Tuckerman, *Chem. Rev.*, 2010, **110**, 2174–2216.
- 8 A. Hassanali, M. K. Prakash, H. Eshet and M. Parrinello, *Proc. Natl. Acad. Sci. U.S.A.*, 2011, **108**, 20410–20415.

- 9 M. Chen, L. Zheng, B. Santra, H.-Y. Ko, R. A. D. Jr, M. L. Klein, R. Car and X. Wu, *Nat. Chem.*, 2018, **10**, 413–419.
- 10 T. J. F. Day, U. W. Schmitt and G. A. Voth, *J. Am. Chem. Soc.*, 2000, **122**, 12027–12028.
- 11 S. T. Roberts, P. B. Petersen, K. Ramasesha, A. Tokmakoff, I. S. Ufimtsev and T. J. Martinez, *Proc. Natl. Acad. Sci. U.S.A.*, 2009, **106**, 15154–15159.
- 12 R. Biswas, Y.-L. S. Tse, A. Tokmakoff and G. A. Voth, *J. Phys. Chem. B*, 2016, **120**, 1793–1804.
- 13 M. E. Tuckerman, A. Chandra and D. Marx, *Acc. Chem. Res.*, 2006, **39**, 151–158.
- 14 Y. Marcus and G. Hefter, *Chem. Rev.*, 2006, **106**, 4585–4621.
- 15 S. V. Guaitolini and J. F. Fardin, *Advances in Renewable Energies and Power Technologies*, Elsevier, 2018, pp. 123 – 150.
- 16 V. Rozsa, D. Pan, F. Giberti and G. Galli, *Proc. Natl. Acad. Sci. U.S.A.*, 2018, **115**, 6952–6957.
- 17 C. Zhang, J. Hutter and M. Sprik, *J. Phys. Chem. Lett.*, 2019, **10**, 3871–3876.
- 18 W. Zhang and A. C. T. van Duin, *J. Phys. Chem. C*, 2015, **119**, 27727–27736.
- 19 J. Behler and M. Parrinello, *Phys. Rev. Lett.*, 2007, **98**, 146401.
- 20 M. Hellström and J. Behler, *J. Phys. Chem. Lett.*, 2016, **7**, 3302–3306.
- 21 S. Plimpton, *J. Comput. Phys.*, 1995, **117**, 1–19.
- 22 A. Singraber, J. Behler and C. Dellago, *J. Chem. Theory Comput.*, 2019, **15**, 1827–1840.
- 23 R. H. Perry, D. W. Green and J. O. Maloney, *Perry's Chemical engineers' handbook*, McGraw-Hill, New York, 6th edn, 1984.
- 24 G. Bussi, D. Donadio and M. Parrinello, *J. Chem. Phys.*, 2007, **126**, 014101.
- 25 M. Hellström, M. Ceriotti and J. Behler, *J. Phys. Chem. B.*, 2018, **122**, 10158–10171.
- 26 H. W. Kuhn, *Nav. Res. Logist. Q.*, 1955, **2**, 83–97.
- 27 J. P. Hansen and I. R. McDonald, *Phys. Rev. A*, 1975, **11**, 2111–2123.
- 28 E. C. Zhong and H. L. Friedman, *J. Phys. Chem.*, 1988, **92**, 1685–1692.
- 29 S. Chowdhuri and A. Chandra, *J. Chem. Phys.*, 2001, **115**, 3732–3741.
- 30 M. P. Allen and D. J. Tildesley, *Computer simulation of liquids*, Oxford university press, 2017.
- 31 J.-M. Caillol, *J. Chem. Phys.*, 1994, **101**, 6080–6090.
- 32 H. K. Kashyap, H. V. R. Annapureddy, F. O. Raineri and C. J. Margulis, *J. Phys. Chem. B*, 2011, **115**, 13212–13221.
- 33 I.-C. Yeh and G. Hummer, *J. Phys. Chem. B*, 2004, **108**, 15873–15879.
- 34 D. Laage and J. T. Hynes, *J. Phys. Chem. B*, 2008, **112**, 7697–7701.
- 35 M. Hellström and J. Behler, *J. Phys. Chem. B*, 2017, **121**, 4184–4190.
- 36 Y. Shao, K. Shigenobu, M. Watanabe and C. Zhang, *chemRxiv.8217152.v2*, 2019.

Supporting information for: Temperature effects on the ionic conductivity in concentrated alkaline electrolyte solutions

Yunqi Shao,[†] Matti Hellström,^{‡,¶} Are Yllö,[†] Jonas Mindemark,[†] Kersti
Hermansson,[†] Jörg Behler,[‡] and Chao Zhang^{*,†}

[†]*Department of Chemistry-Ångström Laboratory, Uppsala University, Lägerhyddsvägen 1,
BOX 538, 75121 Uppsala, Sweden*

[‡]*Universität Göttingen, Institut für Physikalische Chemie, Theoretische Chemie,
Tammannstr. 6, 37077 Göttingen, Germany*

[¶]*Software for Chemistry and Materials B.V., De Boelelaan 1083, 1081HV Amsterdam,
The Netherlands*

E-mail: chao.zhang@kemi.uu.se

Finite-size correction to the Nernst-Einstein conductivity

As is discussed in the main text, the Nernst-Einstein conductivity is computed from the self-diffusion coefficients of cation D_+ and anion D_- (Eq. 1).

$$\sigma_{\text{N-E}} = q^2 \rho \beta (D_+ + D_-) \quad (1)$$

The self-diffusion coefficients with periodic boundary conditions are known to have system-size dependence.^{S1} The dependence is mainly due to the periodicity-induced hydrodynamic

self-interaction which can be corrected using Eq. 2, where D_0 is corrected self-diffusion coefficient, D_{PBC} is the self-diffusion coefficient obtained under periodic boundary conditions (PBC), $\xi \approx 2.837297$ for cubic simulation boxes is a constant determined by the shape of the simulation box, L is the length of the simulation box, β is the inverse temperature and η is the shear viscosity.

$$D_0 = D_{\text{PBC}} + \frac{\xi}{6\pi\beta\eta L} \quad (2)$$

We estimated the finite size effect for the Nernst-Einstein conductivity using Eq 2 and experimental viscosity from Ref. S2. As is shown in Fig. S1, the finite-size correction is rather small compared to the deviation of $\sigma_{\text{N-E}}$ from $\sigma_{\text{G-K}}$ or $\sigma_{\text{Exp.}}$ because of the relatively large simulation box that we used and high viscosity of NaOH solutions. Therefore, we have neglected the finite-size correction and used the uncorrected self-diffusion coefficient and Nernst-Einstein conductivity in Fig.1 shown in the Main Text.

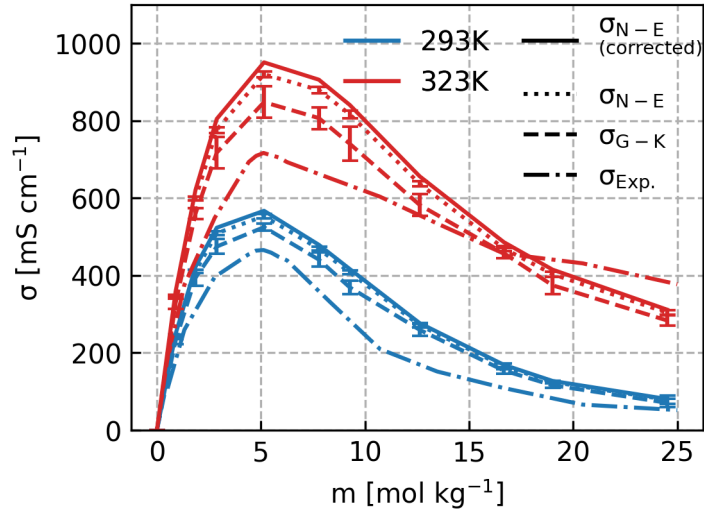


Figure S1: Ionic conductivities of NaOH solutions at 293K and 323K calculated from the Nernst-Einstein formula with and without the finite-size correction, and that obtained from Green-Kubo formula and experimental measurements.

Concentration-dependence of viscosity in NaOH solutions at 293K and 323K from experiments

As seen in Fig. S2a, the viscosity of NaOH solution increases rapidly with the concentration and its value is higher at 293K.

It is interesting to note that deviations from the Nernst-Einstein relation ($\sigma_{N-E} - \sigma_{G-K}$) with a maximum around 5m are larger at 323K than those at 293K (Fig. S1). This is in accord with the concentration-weighted inverse viscosity (see Fig. S2b), in the spirit of the Walden's rule.^{S3}

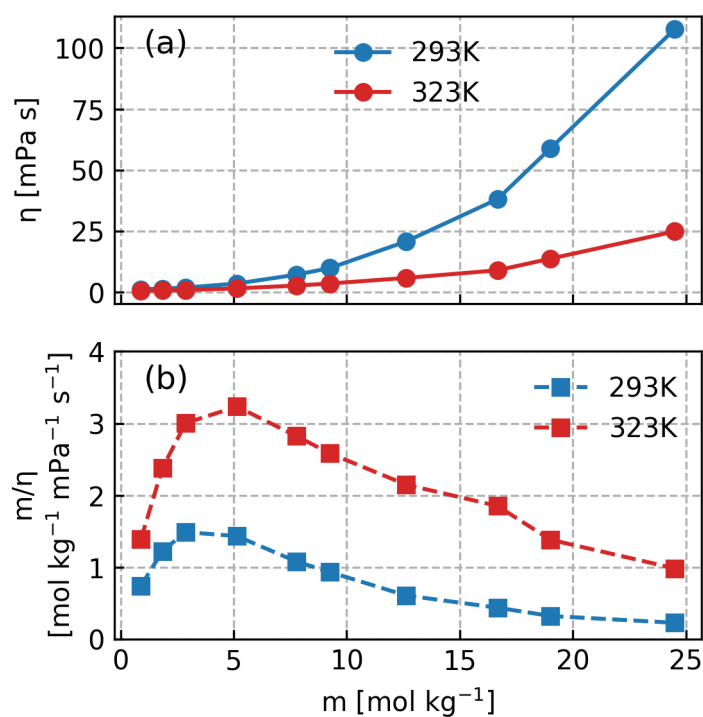


Figure S2: a) Concentration-dependent viscosities of NaOH solutions at 293K and 323K from experimental Ref. S2; b) The corresponding concentration-weighted inverse viscosities at 293K and 323K.

Stoichiometry of simulation boxes

The different molalities of NaOH solutions considered in this work and the actual number of molecules used in the simulations are given in Table S1.

Table S1: Compositions of simulated NaOH solutions in this work: Molality m , number of NaOH and H₂O molecules N_{NaOH} and $N_{\text{H}_2\text{O}}$, length of the cubic simulation box L and density ρ at 293K and 323K.

m [mol/kg]	N_{NaOH}	$N_{\text{H}_2\text{O}}$	$L_{293\text{K}}$ [Å]	$\rho_{293\text{K}}$ [g cm ⁻³]	$L_{323\text{K}}$ [Å]	$\rho_{323\text{K}}$ [g cm ⁻³]
0.896	8	496	24.56	1.04	24.66	1.02
1.852	16	480	24.30	1.07	24.40	1.06
2.874	24	464	24.05	1.11	24.16	1.10
5.144	40	432	23.59	1.19	23.70	1.17
7.778	56	400	23.18	1.26	23.29	1.24
9.259	64	384	22.99	1.30	23.10	1.28
12.626	80	352	22.64	1.36	22.75	1.35
16.667	96	320	22.34	1.43	22.45	1.41
19.006	104	304	22.21	1.46	22.32	1.44
24.509	120	272	21.96	1.52	22.07	1.50

References

- (S1) Yeh, I.-C.; Hummer, G. System-size dependence of diffusion coefficients and viscosities from molecular dynamics simulations with periodic boundary conditions. *J. Phys. Chem. B* **2004**, *108*, 15873–15879.
- (S2) Common Fluid Pumping Sodium Hydroxide with Liquiflo Gear Pumps. 2016; <http://www.liquiflo.com/v2/files/pdf/applicationnotes/AN0101-1-SodiumHydroxide-Jan2016.pdf>.
- (S3) Shao, Y.; Shigenobu, K.; Watanabe, M.; Zhang, C. Role of Viscosity in Deviations from the Nernst-Einstein Relation. *chemRxiv.8217152.v2* **2019**,